11th World Congress on Computational Mechanics (WCCM XI)
5th European Conference on Computational Mechanics (ECCM V)
6th European Conference on Computational Fluid Dynamics (ECFD VI)
E. Oñate, J. Oliver and A. Huerta (Eds)

XFEM FOR A CRACK MODEL WITH STRIP-YIELD CRACK TIP PLASTICITY

K. Kunter*[1], T. Heubrandtner[1], B. Suhr[1] and R. Pippan[2]

[1] VIRTUAL VEHICLE Research Center, Inffeldgasse 21/A, Graz, Austria,
karlheinz.kunter@v2c2.at, http://www.v2c2.at
[2] Erich Schmidt Institute of Materials Science (ESI ÖAW), Leoben, Austria.
reinhard.pippan@oeaw.ac.at, http://www.esi.oeaw.ac.at

Key words: XFEM, cohesive crack, Dugdale model, analytical solution

Abstract. In this paper a simulation method for a strip-yield crack model applied to thin walled structures is presented. For this model an exact analytic solution of the governing differential equations including the inner boundary conditions is known. This analytic solution is reformulated to be useable in the XFEM approach as crack tip enrichment function. The proposed computational method is validated on a single edge cracked specimen againt a high resolution standard FE simulation. Results are in good agreement.

1 INTRODUCTION

The explicit Finite Element (FE) Method is a well established tool for the simulation of dynamic processes in the field of mechanical engineering. For many applications, e.g. the calculation of deformations and intrusions in automotive crash simulations, an acceptable accuracy can be achieved using coarse meshes. However for the numerical analysis of phenomena involving discontinuities, singularities or high gradients, e.g. failure of joints, crack initiation and propagation, the classic FE method needs locally high refined meshes. According to the Courant-Friedrich-Levy criterion this leads to small time steps and thus to unacceptable long computation times, otherwise instabilities will occur.

To overcome these problems many different numerical approaches were developed, e.g. meshless methods, cracking particles method or generalized finite element methods. In [**?**] a review of computational methods for fracture in brittle and quasi-brittle solids can be found. A very popular tool for the simulation of fracture is the extended finite element method (XFEM), which was introduced in [**?**]. In this method elements near the crack are enriched by additional shape functions through the partition of unity concept. Usually this is done in two ways. Elements cut by the crack are enriched with Heaviside functions to allow a discontinuity in the displacement field within an element. Thus a crack can

propagate freely in the mesh without alignment and no prescription of the crack path is necessary. Elements near to the crack tip are enriched with tip enrichment functions. In the ideal case these functions span the analytical solution of the problem, e.g. for brittle fracture the analytical solution of [**?**] is widely used with XFEM. The use of the analytic solution results in higher accuracy then the standard FEM and thus a coarser mesh can be used for XFEM. This is not necessarily the case when the enrichment differs from the analytical solution. The crack representation itself can be chosen independently from the XFEM method, common choices are crack representations as straight line segments or level set methods which also allow curved cracks, when quadratic finite elements are used (compare [**?**]). Between tip enriched and standard elements the so-called blending elements are placed. Here a special treatment can help to avoid unwanted terms at the boundary between enriched and not enriched elements, see [**?**]. The integration of enriched elements needs to be treated with care. Sub-triangulation of elements cut by the crack or containing the crack tip is needed together with an adaption of the degree of the quadrature rule. Especially in 3d this is a major task. It should be noted, that the XFEM approach is well suited for a small number of cracks while the handling of many cracks becomes cumbersome.

Strip-yield models, also often called cohesive models, introduced by Baerenblatt [**?**] and Dugdale [**?**], are widely used for the simulation of cracks in quasi-brittle materials. They avoid the use of nonlinear material models but still describe plasticity effects of the material. The crack is virtually extended with a strip-yield zone, where a non-vanishing traction acts. While the original crack remains traction free, the non-vanishing traction in the strip-yield zone represents the hardening and softening of the material. Strip-yield models can be efficiently simulated using XFEM. In [**?**, **?**] Xiao and Karihaloo derived asymptotic fields for several cohesive laws under mixed-mode conditions and used them in XFEM simulations. The traction of the asymptotic fields used as tip enrichment equals asymptotically the predefined closure stress in the cohesive zone. On the remaining crack the faces are not traction free. In this paper the exact analytical solution of the strip-yield model will be used as tip enrichment in the XFEM approach. This analytical solution, derived in [**?**], equals exactly the predefined closure stress in the strip-yield zone and is traction free on the rest of the crack.

This paper is organized as follows. In section 2 the problem setting and a summary of the derivation of the analytical solution will be given, for details see [**?**]. To use the analytic solution as crack tip enrichment it needs to be reformulated. Section 3 describes the use of this solution in the XFEM approach and the computational method for the strip-yield model. Section 4 contains the validation of the proposed method. The solution of a single edge cracked specimen is compared to a high resolution FE simulation. In section 5 conclusions are drawn.

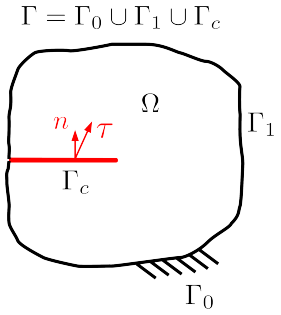

Figure 1: Illustration of the solution domain Ω with the outer boundary $\Gamma_0 \cup \Gamma_1$ and the crack Γ_c.

2 PROBLEM SETTING AND ANALYTICAL SOLUTION

We denote by Ω the general solution domain in 2d, which contains a sharp crack, Γ_C (see fig. 1). A Dirichlet, i.e. displacement, boundary condition is applied on Γ_0 and a Neumann, i.e. force, boundary condition on Γ_1, where $\Gamma = \Gamma_C \cup \Gamma_0 \cup \Gamma_1$. We consider a plane stress problem within the framework of small displacements. The material is linear elastic and no volume forces are present.

The strip-yield model, which we consider, was first introduced by [**?**, **?**] for a through crack in an infinite plate for a non-hardening material in plane stress. The elastic-plastic behavior is approximated by the superposition of the linear elastic solution for traction free crack edges and a solution for a closure stress with a magnitude of the yield stress σ_y at the crack tip such that the stress singularity of the linear elastic near field solution is removed.

Fig. 2 shows a Dugdale-like configuration (Mode I). A crack ranges from $-\infty$ to $+r_D$ on the x-axis, where for $0 < x < r_D$ (in the Dugdale zone) a constant crack closing traction $\hat{\tau} = \pm\, i\, \hat{\tau}_D$ ($\hat{\tau}_D \in \mathbb{R}$) acts. The rest of the crack, i.e. for $x \leq 0$, is traction free.

Throughout this paper the complex derivative is denoted by $(\cdot)'$, the complex conjugate by $\overline{(\cdot)}$ and the adjoint (conjugate and transpose) by $(\cdot)^* := \overline{(\cdot)}^T$. The two holomorphic complex potentials, $\phi(z)$ and $\psi(z)$, and their complex derivatives are related to the general solution for the displacement- and stress-fields [**?**, **?**, **?**] as follows:

$$q = \frac{1}{2\mu}\left(\kappa\phi(z) - z\overline{\phi'(z)} - \overline{\psi(z)}\right) , \tag{1}$$

$$\sigma_h = \phi'(z) + \overline{\phi'(z)} , \qquad \sigma_d = z\overline{\phi''(z)} + \overline{\psi'(z)} , \tag{2}$$

where $\kappa = (3-\nu)/(1+\nu)$ for plane stress, with Poisson's ratio $\nu = \lambda/(2(\lambda+\mu))$, and λ and μ are the Lame constants. The quantities, σ_h and σ_d, are the stress combinations introduced by Kolosov [**?**].

A comprehensive description of the derivation of the analytical solution can be found in [**?**]. Here we present a short summary. We construct the analytical solution in the crack tip region, which will satisfy the governing partial differential equations as well as the inhomogeneous traction boundary conditions imposed by the Dugdale model.

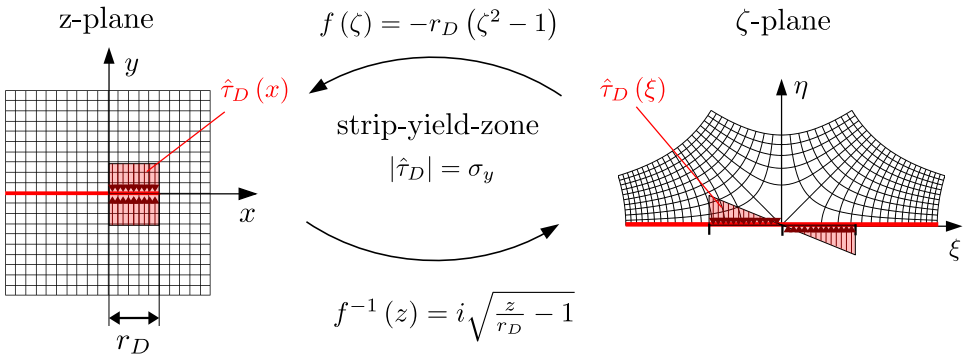

Figure 2: Mapping of the physical solution domain in the complex z-plane to the upper half plane (ζ-plane) by a conformal mapping function $f(\zeta) = -r_D(\zeta^2 - 1)$. The physical solution domain contains a straight crack along the negative part of the x-axes with a physical crack tip at $x = y = 0$ and a leading strip yield zone of length r_D, where a traction $\hat{\tau}$ with magnitude of the materials yield stress σ_y acts.

2.1 Calculation of the complex potentials, ϕ and ψ

For convenience we introduce a conformal mapping (see fig. 2), which maps the physical z-plane to the upper half of the complex plane ζ by means of the holomorphic inverse function $f^{-1}(z) = \zeta$, where

$$z = f(\zeta) = -r_D(\zeta^2 - 1) \ . \tag{3}$$

The crack is mapped on the real ξ-axis in the ζ-plane, such that the Dugdale-zone is located in the interval $(-1, 1)$. If we choose ψ as a function of ϕ in the following way,

$$\psi(\zeta) = -\overline{\phi(\overline{\zeta})} - \frac{\overline{f(\overline{\zeta})}}{\dot{f}(\zeta)}\dot{\phi}(\zeta) \ , \tag{4}$$

then the boundary condition can be formulated as follows

$$\left[\phi(\zeta) - \phi(\overline{\zeta})\right]_{\zeta=\xi^+} = \begin{cases} \hat{\tau}_D f(\xi) & \text{for } |\xi| < 1 \\ 0 & \text{for } |\xi| \geqslant 1 \end{cases} \ , \tag{5}$$

in which the substitution $\zeta = \xi^+$ means that ζ and $\overline{\zeta}$ approach the real ξ-axis from the upper and lower half plane, respectively. A dot over an expression means derivation with respect to ζ. A solution of (5) can be found with the representation for ϕ

$$\phi(\zeta) = \underbrace{\sum_{k=0}^{K} A_k \zeta^k}_{=:\phi_h} + \underbrace{\sum_{n=1}^{\infty} a_n \hat{W}_n(\zeta)}_{=:\phi_p} \ , \tag{6}$$

where the homogeneous part, $\phi_h(\zeta)$, is a power series with complex coefficients, A_k, so that (5) reduces to

$$\left[\phi_p(\zeta) - \phi_p(\overline{\zeta})\right]_{\zeta=\xi^+} = \begin{cases} \hat{\tau}_D f(\xi) & \text{for } |\xi| < 1 \\ 0 & \text{for } |\xi| \geqslant 1 \end{cases} \ . \tag{7}$$

For the inhomogeneous part, $\phi_p(\zeta)$, a more specific representation is chosen by means of a series of base functions

$$W_n(\zeta) = \left(\zeta - \sqrt{\zeta^2 - 1}\right)^n , \tag{8}$$

with complex coefficients, a_n. Each function $W_n(\zeta)$ consists of two Riemann sheets from which we use the one that approaches zero for $|\zeta| \to \infty$. We chose the branch cut on the real ξ-axis that connects the two branch points at ± 1. Due to this construction, the boundary condition outside of the Dugdale zone, $|\xi| \geqslant 1$, is already fulfilled. Suitable coefficients a_n have to be found, such that the condition inside the Dugdale zone, $|\xi| < 1$, is also met, and we get

$$a_n = -\frac{4i}{\pi}\,\hat{\tau}_D\, r_D \begin{cases} \frac{1}{n(n^2-4)} & \text{for odd } n \\ 0 & \text{for even } n \end{cases} . \tag{9}$$

By inserting (9) and (8) in (6) we finally obtain the closed form,

$$\phi_p(\zeta) = \frac{i}{\pi}\hat{\tau}_D r_D \left(\zeta - 2\left(\zeta^2 - 1\right)\tanh^{-1}\left(\zeta - \sqrt{\zeta^2 - 1}\right)\right) , \tag{10}$$

for the inhomogeneous part $\phi_p(\zeta)$ in case of a constant traction density.

The homogeneous part of $\phi(\zeta)$ causes a singularity in the stress field at the crack tip, which needs to be removed by the inhomogeneous part. Calculating the limit of the von Mises-stress for $z \to r_D$ the following required relation between the coefficient A_1 and the length of the Dugdale-zone r_D is found,

$$r_D = \frac{i\pi}{2\hat{\tau}_D} A_1 . \tag{11}$$

2.2 Analytical solution as crack tip enrichment

The obtained analytical solution needs to be reformulated such that it can be used as tip enrichment functions in the XFEM formalism. The complex displacement as stated in eq. (1) can be written in the following form, using (4) for ψ, (6) for ϕ_h and (10), (11) for ϕ_p:

$$\begin{aligned} q(\zeta) = &\sum_{k=1}^{K} \underbrace{\frac{1}{2\mu}\kappa\zeta^k}_{=:g_1^k(\zeta)} A_k + \sum_{k=1}^{K} \underbrace{\frac{1}{2\mu}\overline{\zeta^k}}_{=:g_2^k(\zeta)} A_k + \sum_{k=1}^{K} \underbrace{\frac{1}{2\mu}\frac{f(\overline{\zeta}) - f(\zeta)}{\overline{\dot{f}}(\zeta)} k\overline{\zeta}^{k-1}}_{=:g_3^k(\zeta)} \overline{A_k} \\ &+ \underbrace{\left(\frac{1}{2\mu}\kappa\phi_p^A(\zeta) + \phi_p^A(\overline{\zeta})\right)}_{=:g_4^k(\zeta)} A_1 + \underbrace{\left(\frac{1}{2\mu}\frac{f(\overline{\zeta}) - f(\zeta)}{\overline{\dot{f}}(\zeta)}\overline{\dot{\phi}_p^A}(\zeta)\right)}_{=:g_5^k(\zeta)} \overline{A_1} , \end{aligned} \tag{12}$$

where $\phi_p^A(\zeta) := -0.5\left(\zeta - 2\left(\zeta^2 - 1\right)\tanh^{-1}\left(\zeta - \sqrt{\zeta^2 - 1}\right)\right)$. The coefficients A_k are complex numbers and can be represented as $A_k = \alpha_k + i\beta_k$ with $\alpha_k, \beta_k \in \mathbb{R}$. Now the

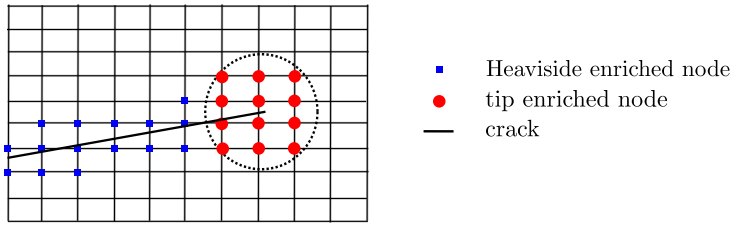

Figure 3: Illustration of XFEM enrichment strategy: nodes near the crack tip are enriched with tip enrichment functions, while nodes belonging to elements cut by the crack are enriched with the Heaviside function.

two dimensional real displacement (u_1, u_2) can be expressed using the real and imaginary part of the complex displacement q.

$$\begin{pmatrix} u_1(f(\zeta)) \\ u_2(f(\zeta)) \end{pmatrix} = \sum_{k=1}^{K} \begin{bmatrix} f_{11}^k(\zeta) & f_{12}^k(\zeta) \\ f_{21}^k(\zeta) & f_{22}^k(\zeta) \end{bmatrix} \begin{pmatrix} \alpha_k \\ \beta_k \end{pmatrix} , \tag{13a}$$

$$f_{11}^k(\zeta) = \mathrm{Re}\Big(g_1^k(\zeta) + g_2^k(\zeta) + g_3^k(\zeta) + \delta_{1k} \left(g_4^k(\zeta) + g_5^k(\zeta) \right) \Big) \tag{13b}$$

$$f_{12}^k(\zeta) = \mathrm{Re}\Big(i \Big[g_1^k(\zeta) + g_2^k(\zeta) - g_3^k(\zeta) + \delta_{1k} \left(g_4^k(\zeta) - g_5^k(\zeta) \right) \Big] \Big) \tag{13c}$$

$$f_{21}^k(\zeta) = \mathrm{Im}\Big(g_1^k(\zeta) + g_2^k(\zeta) + g_3^k(\zeta) + \delta_{1k} \left(g_4^k(\zeta) + g_5^k(\zeta) \right) \Big) \tag{13d}$$

$$f_{22}^k(\zeta) = \mathrm{Im}\Big(i \Big[g_1^k(\zeta) + g_2^k(\zeta) - g_3^k(\zeta) + \delta_{1k} \left(g_4^k(\zeta) - g_5^k(\zeta) \right) \Big] \Big) \tag{13e}$$

where δ_{ij} is the Kronecker delta. With eq. (13) we found a form of the analytic solution which can be used in the XFEM approach, which will be described in the following section.

3 COMPUTATIONAL APPROACH USING XFEM

For the XFEM formalism nodes near the crack are enriched with additional shape functions. Nodes of elements which are cut by the crack are enriched with the Heaviside function, such that the displacement includes a jump over the crack. Nodes near the crack tip are enriched with crack tip enrichment functions.

3.1 Enrichment functions and strategies

In this paper we choose to enrich all nodes whose distance to the crack tip is below a given radius. Other enrichment strategies are possible and can be found in the literature. Fig. 3 illustrates the setting. We denote by I the set of indices of all nodes, by I_H indices of Heaviside enriched nodes and by I_T indices of tip enriched nodes. Then the XFEM approach for the displacement is as follows:

$$\begin{pmatrix} u_1 \\ u_2 \end{pmatrix}(x) = \sum_{i \in I} \phi_i(x) \begin{pmatrix} u_1^i \\ u_2^i \end{pmatrix} + \sum_{j \in I_H} \phi_j(x) H(x) \begin{pmatrix} \gamma_1^j \\ \gamma_2^j \end{pmatrix} + \sum_{l \in I_T} \phi_l(x) \sum_{k=1}^{K} \begin{bmatrix} f_{11}^k & f_{12}^k \\ f_{21}^k & f_{22}^k \end{bmatrix} (\zeta) \begin{pmatrix} \alpha_k^l \\ \beta_k^l \end{pmatrix} , \tag{14}$$

where $\phi_i(x)$ is the standard FE shape function belonging to node i and $\zeta = f^{-1}(x)$ defined as depicted in fig. 2. In addition to the standard degree of freedoms u_1^i, u_2^i, new degrees of freedom γ_1^j, γ_2^j associated with the jump enrichment and α_k^l, β_k^l associated with the tip enrichment are introduced. In the elements which contain the crack tip and the Dugdale zone all nodes are constrained to have the same α_k, β_k for each order.

3.2 Principle of virtual work

In the next step we state the equation of virtual work for our problem and use the above ansatz, eq. (14), for the displacement. Note that this approach is equivalent to the mathematical weak formulation of the boundary value problem followed by the Galerkin method. For the displacement u as well as for the test function v the ansatz of eq. (14) is used

$$\int_\Omega \boldsymbol{M}\epsilon(u) : \epsilon(v)\, dx + \int_{\Gamma_D} \sigma_y \cdot w(v)\, do = \int_{\Gamma_1} F \cdot v\, do\,, \tag{15}$$

where Γ_D denotes the Dugdale zone, $\epsilon(u)$ is the strain tensor, $\boldsymbol{M} \in \mathbb{R}^{3\times 3}$ is the elasticity tensor for the plane stress case, such that $\sigma(u) = \boldsymbol{M} \cdot \epsilon(u)$, $w(v)$ denotes the jump of the test function v over the crack and for two tensors a and b, $a : b := \sum_{i,j} a_{ij} b_{ij}$ is the sum of the component wise multiplication.

For enriched nodes the strain tensor and thus the derivatives of the enrichment functions have to be calculated. While this is easy for the Heaviside enrichment, care has to be taken for the crack tip enrichment functions. Here the derivation in the x, y plane is transformed to complex derivatives.

Eq. (15) then results in a system of equations for the degrees of freedom of the displacement $u_1^i, u_2^i, \gamma_1^j\, \gamma_2^j, \alpha_k^l, \beta_k^l$. Due to the conformal mapping, introduced in eq. (3), this system of equations contains a nonlinear dependence of the length of the Dugdale zone, r_D. For a given external load, r_D is slowly increased until the degrees of freedom of the displacement remain unchanged. This can be considered as a fixed point problem for the degrees of freedom, while it is computationally more efficient to reformulate this problem using a damped quasi-Newton method.

The implementation is based on a freely available XFEM implementation [**?**, **?**]. Cracks are represented as straight line segments and the mentioned constraining of the crack tip enrichment is implemented as penalty formulation.

3.3 Projection of the stress tensor

There are several possible scenarios where an accurate determination of the stress close to the crack tip is of high importance. Crack propagation can be one of these cases. In the standard FE method the stress calculated from the displacement via derivation is discontinuous at the element boundaries. We call this quantity the compatible stress. In the literature different approaches can be found how to increase the accuracy of the compatible stress near the crack tip. The application of moving least squares (MLS)

smoothing or averaging in a post processing is a simple way to a obtain a continuous stress, but can lead to problems such as unwanted oscillations. In [**?**] a statically admissible stress recovery scheme is derived, where the stress is fitted at sampling point to basis functions, which fulfill the equilibrium condition in the domain and the traction condition on the boundary. In contrast to methods which act as post processing routines there exist approaches, which alter the enrichement functions to achieve a higher accuracy in the compatible stress, see e.g. [**?**].

In this paper the stress tensor is projected in a L^2-sense on the analytical solution. This approach is also a post processing method and therefore easy to add to an existing implementation. The projection is applied only for elements which contain tip enriched nodes, i.e. fully tip enriched elements and blending elements. We denote the domain of projection by Ω_{enr}. Here the compatible stress is projected on the analytical solution, which is given by

$$\begin{pmatrix} \sigma_x^{analytic} \\ \sigma_y^{analytic} \\ \tau_{xy}^{analytic} \end{pmatrix}(x)\Big|_{\Omega_{enr}} = \boldsymbol{M}\left(\sum_{j\in I\setminus I_T} \epsilon(\phi_j)(x) + \sum_{l\in I_T} \phi_l(x) \sum_{k=1}^{K} \begin{bmatrix} \frac{\partial f_{11}^k}{\partial x} & \frac{\partial f_{12}^k}{\partial x} \\ \frac{\partial f_{21}^k}{\partial y} & \frac{\partial f_{22}^k}{\partial y} \\ \frac{\partial f_{11}^k}{\partial x} + \frac{\partial f_{21}^k}{\partial y} & \frac{\partial f_{12}^k}{\partial x} + \frac{\partial f_{22}^k}{\partial y} \end{bmatrix}(\zeta) \begin{pmatrix} \hat{\alpha}_k^l \\ \hat{\beta}_k^l \end{pmatrix} \right), \tag{16}$$

where $\zeta = f^{-1}(x)$. The projection in L^2-sense is conducted by solving the resulting system of equations for the new coefficients $u_1^j, u_2^j, \hat{\alpha}_k^l, \hat{\beta}_k^l$:

$$\int_{\Omega_{enr}} \sigma^{analytic}(x) : \sigma^{analytic}(x) dx = \int_{\Omega_{enr}} \sigma(x) : \sigma^{analytic}(x) dx \,, \tag{17}$$

where $\sigma^{analytic}$ denotes the analytic stress tensor and σ the compatible stress tensor.

4 NUMERICAL EXAMPLE – VALIDATION

For the validation of our presented approach we consider a specimen with a single edge crack. The resulting length of the Dugdale zone and the calculated stress field will be compared against a high resolution standard FE simulation.

The specimen is of height $2h$ and width w, where $h = w = 60mm$ is chosen. The thickness of the specimen is $t = 1.5mm$ and the existing crack is of length $c = 8mm$, see fig. 4. At the upper and lower edge of the specimen a symmetric displacement boundary condition is applied, $v = \pm(0, 0.05mm)$. The material parameters are the E-modulus $E = 205GPa$ and the Poisson number $\nu = 0.3$. In the Dugdale zone a constant traction of $\hat{\tau}_D = 400MPa$ is applied.

For the XFEM calculation a mesh with nearly quadratic elements with an edge length of $\approx 3mm$ are chosen. For the crack tip enrichment a radius of $7.5mm$ is chosen. The crack tip enrichment functions are chosen to be of order three, i.e. $K = 3$ in eq. (14). For the validation a standard FE simulation with a mesh of edge length $0.1mm$ is conducted.

Both the standard FE as well as the XFEM simulation return a length of the Dugdale zone of $3.2mm$. Fig. 5 shows a comparison of the von Mises stress near the crack tip

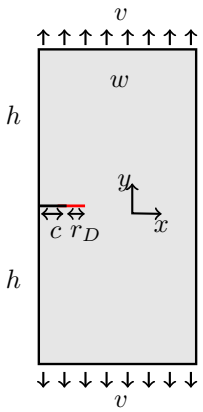

Figure 4: Validation setting: A single edge cracked specimen of width w and height $2h$ contains a crack of length c and a strip yield zone of length r_D. A symmetric displacement boundary condition of magnitude v is applied at the lower and the upper edge.

between the standard FE and the XFEM simulation. Within the enriched domain the XFEM stress is projected on the analytic solution. In the fully tip enriched elements a good agreement with the FE results is obtained. Due to the partial enrichments in the blending elements, a perturbation is introduced. This leads to big deviation between the FE and XFEM results in the blending elements. To improve the XFEM results in the blending elements an approach as suggested in [**?**] combined with an adapted stress projection could be used.

For a better comparison between the standard FE and the XFEM, the von Mises stress, as well as the σ_{xx} and σ_{yy} components of the stress tensor are plotted. Fig. 6 shows the stress on the upper crack edge within the fully tip enriched domain. The real crack tip, i.e. the end of the traction free crack is placed at $8mm$. The Dugdale zone with the prescribed traction of $400MPa$ ranges from $8mm$ to $11.2mm$. Both the FE and the XFEM results agree well in the σ_{yy} component with the prescribed boundary conditions. Fig. 7 shows the stress on a line normal to the crack, also in the fully tip enriched domain. Here it can be seen that the stress calculated by XFEM declines slightly stronger than the one calculated by FE. This might be connected to the chosen stress projection. In general it can be said that both calculated stress agrees very well in the vicinity of the crack tip, i.e. in the fully tip enriched domain.

5 CONCLUSIONS

Considering a strip-yield crack model applied to thin walled structures a computational approach is developed. Starting from the known exact analytical solution, see [**?**], the XFEM method is applied. The analytical solution is reformulated to be usable as crack tip enrichment. A validation is conducted on a single edge cracked specimen against, comparing the XFEM solution with a high resolution standard FE simulation. Results are in good agreement.

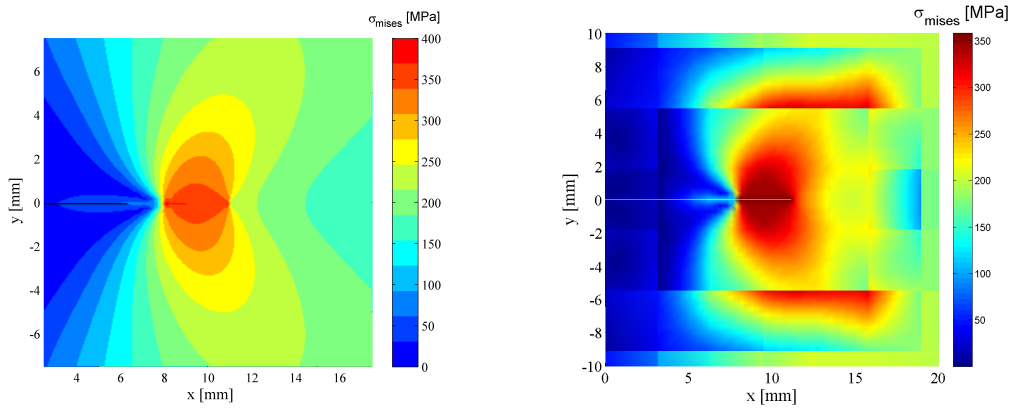

Figure 5: Von Mises Stress in the vicinity of the crack tip. Left: FE Simulation, Right: XFEM simulation.

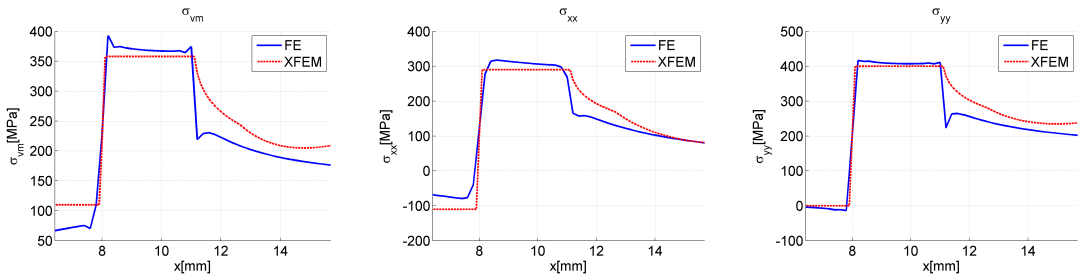

Figure 6: Comparison of the stress computed by FE and XFEM on the axis on the crack plane ($y = 0mm$).

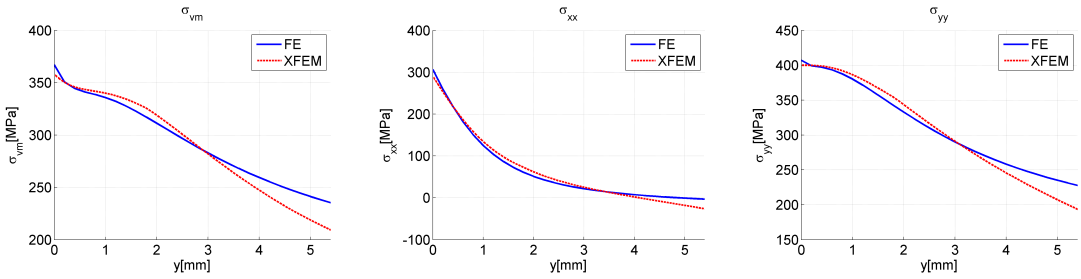

Figure 7: Comparison of the stress computed by FE and XFEM along a line normal to the crack tip ($x = 10mm$).

ACKNOWLEDGMENTS

The authors would like to acknowledge the financial support of the "COMET K2 - Competence Centres for Excellent Technologies Programme" of the Austrian Federal Ministry for Transport, Innovation and Technology (BMVIT), the Austrian Federal Ministry of Economy, Family and Youth (BMWFJ), the Austrian Research Promotion Agency (FFG), the Province of Styria and the Styrian Business Promotion Agency (SFG).
We would furthermore like to express our thanks to our supporting scientific project partner, the Austrian Academy of Science.

REFERENCES

[1] Timon Rabczuk. Computational methods for fracture in brittle and quasi-brittle solids: State-of-the-art review and future perspectives. *ISRN Applied Mathematics*, 2013:38, 2013.

[2] Nicolas Moës, John Dolbow, and Ted Belytschko. A finite element method for crack growth without remeshing. *Int J Numer Meth Eng*, 46(1):131–150, 1999.

[3] M. L. Williams. The bending stress distribution at the base of a stationary crack. *J Appl Mech*, 28:78, 1961.

[4] M. Stolarska, D. L. Chopp, N. Moës, and T. Belytschko. Modelling crack growth by level sets in the extended finite element method. *Int J Numer Meth Eng*, 51(8):943–960, 2001.

[5] Thomas-Peter Fries. A corrected XFEM approximation without problems in blending elements. *Int J Numer Meth Eng*, 75(5):503–532, 2008.

[6] G. I. Barenblatt. The mathematical theory of equilibrium cracks in brittle fracture. *Adv Appl Mech*, VII:63 – 78, 1962.

[7] D. S. Dugdale. Yielding of steel sheets containing slits. *J Mech Phys Solids*, 8(2):100 – 104, 1960.

[8] Q. Z. Xiao and B. L. Karihaloo. Asymptotic fields at frictionless and frictional cohesive crack tips in quasibrittle materials. *J Mech Mater Struct*, 1(5):881 – 910, 2006.

[9] B.L. Karihaloo and Q.Z. Xiao. Asymptotic fields at the tip of a cohesive crack. *International Journal of Fracture*, 150(1-2):55–74, 2008.

[10] K. Kunter, T. Heubrandtner, and R. Pippan. Simulation of crack propagation using hybrid Trefftz method based on a strip-yield crack-tip plasticity model for automotive crash applications. In *Proceedings of the 19th European Conference on Fracture*, 2013.

[11] G. V. Kolosov. *On an application of complex function theory to a plane problem of the mathematical theory elasticity.* Yuriev, 1909.

[12] N. I. Muskhelishvili. *Some Basic Problems on the Mathematical Theory of Elasticity.* Noordhoff, 1952.

[13] A. H. England. *Complex variable methods in elasticity.* Wiley-Interscience, NY, 1971.

[14] S. Bordas, P. V. Nguyen, C. Dunant, A. Guidoum, and H. Nguyen-Dang. An extended finite element library. *Int J Numer Meth Eng*, 71(6):703–732, 2007.

[15] S. Natarajan, S. Bordas, and D. Roy Mahapatra. Numerical integration over arbitrary polygonal domains based on Schwarz-Christoffel conformal mapping. *Int J Numer Meth Eng*, 80(1):103–134, 2009.

[16] Q. Z. Xiao, B. L. Karihaloo, and X. Y. Liu. Incremental-secant modulus iteration scheme and stress recovery for simulating cracking process in quasi-brittle materials using XFEM. *Int J Numer Meth Eng*, 69(12):2606–2635, 2007.

[17] L. Chen, T. Rabczuk, S.P.A. Bordas, G.R. Liu, K.Y. Zeng, and P. Kerfriden. Extended finite element method with edge-based strain smoothing (ESm-XFEM) for linear elastic crack growth. *Comput Methods Appl Mech Engrg*, 209 - 212(0):250 – 265, 2012.